CHEMICAL ENGINEERING TRANSACTIONS
VOL.
A publication of AIDIC
The Italian Association of Chemical Engineering
Online at www.cetjournal.it
Guest Editors:

ISSN 2283-9216

Evaluation of the Induced Oil Remobilization through High and Low Salinity Waterflooding in a Porous System Via X-Ray Microtomography

Anderson C. Moreira*, Verônica A. Santos, Iara F. Mantovani, José A.B. Cunha Neto, Celso P. Fernandes

Federal University of Santa Catarina (UFSC), Department of Mechanical Engineering (EMC/PGMAT), Laboratory of Porous Media and Thermophysical Properties (LMPT), Zipcode 88040 900 Florianópolis, SC, Brazil
*anderson@lmpt.ufsc.br

The X-ray microtomography was used to visualize and characterize the remobilization oil process inside the porous system of a carbonate rock sample. After being saturated with a brine solution, dodecane oil was injected into the porous media, initially a predominant water-wet system. After an aging process is performed, the system became mixed-wet. The remobilization was induced by the injection of two KI (Potassium Iodide) brine solutions, a high salinity solution injection (1.5 M) followed by a low one (0.3 M). The intention was to achieve, besides the immiscible displacement process, oil remobilization due to the modification of interfacial properties of fluids and wettability caused by low salinity of the injected brine. It was observed that the low salinity brine was capable of shifting the oil inside the porous medium and reduce the residual oil saturation.

1. Introduction

The study of two-phase immiscible fluids configurations in porous systems, such as water and oil, is of significance in energy and environmental science technologies. Oil and gas production is still an important source of energy for the global transportation system, in which the main issue is the generation of pollutants, such as the formation water (Macheca and Uwiragiye, 2020) and the oil itself. In events of an undesired oil spill, besides polluting seawater, the oil may leak to the ground damaging soil and groundwater reservoirs. In order to reduce the negative impact on the environment, the contaminated water must be treated (Durval et al., 2019) and the oil removed from solid surfaces (Almeida et al., 2019). In the case of solid surfaces, whether to solve problems with contamination (Duffy et al., 1980; Pichtel, 2020) or to improve hydrocarbons recovering techniques (Qin et al., 2019), methodologies aiming to enhance the oil remobilization have been studied.
Immiscible displacement mechanism is used to remove oil via water injection, however, due to heterogeneities of the porous structure some residual oil remains trapped in the medium by capillary forces (Gbadamosi et al., 2019). When this condition is achieved, Enhanced Oil Recovering (EOR) techniques are applied. EOR increases the ability of oil to flow due to modifications on its physical properties caused by thermal, chemical, and miscible processes (Satter and Iqbol, 2016).
The study of EOR processes in laboratory has been supported by the X-ray microtomography (microCT) technique, which enables one to quantify the saturation of fluids inside samples and contributes to the understanding of the oil remobilization mechanisms via image analysis. MicroCT has been used in experiments of EOR with the application of nanoparticles (Pak et al., 2018), microbial products (Armostrong and Wildenschild, 2012), oil-in-water emulsion (Scheffer et al., 2020), polymer flooding (Wenguo, 2016) and low-salinity aqueous solutions (Bartels et al., 2016), among others.
Low-salinity water injection (LSW) is one EOR technique in which chemical and mechanical effects on oil remobilization are not totally explained yet. According to Katende and Sagala (2019), this is due to the complexity and number of parameters behind crude oil/brine/rock interactions, therefore, more than one

mechanism may influence LSW application. Nevertheless, it is well documented that low salinity increases the oil recovery instead of brine with higher salt concentrations (Katende and Sagala, 2019).
The X-ray microtomography technique was applied in the investigation of the oil remobilization process that took place inside a carbonate rock sample. The remobilization was induced by LSW injection after an immiscible displacement with a higher salt concentration solution was carried out. This study intends to shed light on the mechanisms that evolve the oil remobilization induced by LSW via 2D and 3D image analyses.

2. Low Salinity Water Injection (LSW)

The principles of EOR imply in modify fluids properties aiming to restore oil flow. The alteration of water-oil interfacial tension and changings in the wettability of the system can detach oil from the solid surface inducing remobilization. The mechanisms behind LSW are not fully understood, they depend on the solids surface's lithology, properties of the oleic phase, ionic concentration and ionic composition of the brine, and so on. However, some effects suggested for LSW are the reduction in the interfacial tension induced by alteration on pH values and the dispersion of clay minerals attached to oil negatively charged. More details can be found in Aladasani et al. (2014) and Katende and Sagala (2019).

3. Experimental

3.1 Sample and Fluids

The sample is a carbonate plug taken from an outcrop rock. It is an analogous reservoir, i.e. has the same structural and fluid properties as oil reservoir rocks. The composition of the rock is predominantly calcite (calcium carbonate, $CaCO_3$), and dolomite (calcium magnesium carbonate, $CaMg(CO_3)_2$). The main parameters of the sample are: 15 mm height x 14 mm dimeter; 0.24 porosity; 2.9 10^{-12} m^2 permeability, and 1.08 x 10^{-1} ml pore volume (VP). The oleic phase is a 0.01 M of stearic acid in dodecane oil. The acid induces the system to become more oil-wet. The salt used in aqueous solutions is Potassium Iodide (KI). The concentrations for high and low salinity brines are, respectively, 1.5 M and 0.3 M. A thermal process (aging) was applied to enhance the wettability of the oleic phase.

3.2 LSW Flooding

A homemade flooding cell was used in the experiment. The cell has appropriate tubbing and valves and is made of aluminum, which combines mechanical resistance with minimum absorbance of X-rays. The sample is encapsulated with resin to assure the fluid flow just take a place inside the porous medium. Initially, the sample was saturated with deionized water, and then 1.5 M solution was injected (5 ml) turning the aqueous phase inside sample into KI 1.5 M solution by dilution. The next steps were carried out as follows:

- Two sequential injections of oleic phase; 10 VP / 250 μl/min flow rate followed by 10 VP / 500 μl/min, total injection times of 4.30 min and 2.15 min, respectively. The oil injection ended once water stopped to come out the sample;
- The flooding cell was placed into an oven for aging (70 °C / 96 h);
- Injection of 1.5 M solution of brine (20 VP / 250 μl/min – total injection time ~9 min);
- Injection of 0.3 M solution of brine (20 VP / 250 μl/min– total injection time ~9 min). Both brine injections were performed under capillary dominant flow regime (capillary number ~10^{-7}).

After each of the above cited steps, the sample was imaged with MicroCT.

3.3 MicroCT Images Acquisitions and Processing

X-ray microtomography acquisitions were carried out with a Zeiss/Versa XRM-500 microCT scanner (Mantovani et al., 2019), in two different spatial resolutions; 7 μm/voxel and 15 μm/voxel. Both set of images were denoised, registered, and ternarized into water, oil, and solid phases with Avizo software. For the quantifications 650 out of 1000 2D slices were analysed, 125 slices from the top and from the bottom of the stack were discarded due to the high incidence of Feldkamp artifacts (Villarraga-Gómez and Smith et al., 2015). A cylindrical volume of interest, which perfectly fits the sample was selected, delimiting the volume of analysis.

4. Results and Discussions

The fluid volumes involved in the experiment are very small, the available space for solutions and oil is just 1.08 x 10^{-1} ml (the sample VP). The difficulty of the experiment relies on the volumetric measurement of such small fluid volumes. Therefore, all the measurements were carried out based on image analysis.
The higher is the concentration of the salt the higher is the X-rays attenuation by the aqueous solution, the result is a brighter intensity in the microtomography image. As can be seen in Figure 1, in which the steps of the

experiments after the aging process are shown by means of bidimensional images at the same slice (number 46, z direction), the rock, aqueous solutions, and oil phases can be distinguished by the intensity of the grey level. The pore phase is filled with oil, darker color, and with 1.5 M brine, a brighter intensity, the intermediary grey level denotes the rock (Figure 1 “a” and “b”). After the injection of the low salinity solution (Figure 1c) three fluids occupy the pore phase, in which the 0.3 M brine grey level is just slightly brighter than the oil.

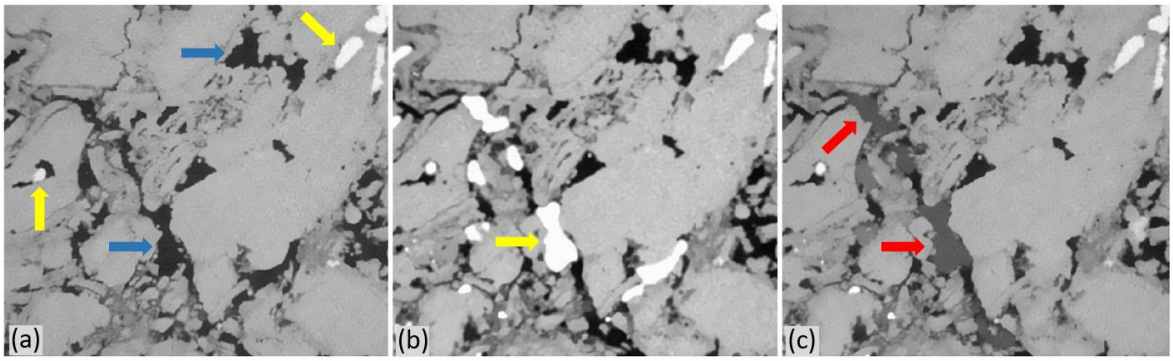

Figure 1: Regions of interest taken from microtomography 2D slices (7 μm/voxel). After the aging (a), most of the pores are filled with oil (dark color-blue arrows) and some are filled with 1.5 M brine (brighter spots-yellow arrows). After the injection of 1.5 M brine (b), the aqueous solution invades more pores of the rock, replacing the oil (yellow arrow). The low salinity solution attenuates less radiation than high salinity, thus the 0.3 M (red arrows) brine (injected after 1.5 M brine solution for EOR purposes) presents a grey level different from 1.5 M brine (c).

After the aging, the sample presents more affinity with oil than with the brine. An indication of the oil wettability is a spreading oil film between the rock and the aqueous solution. In the Figure 2, two regions from other slices are shown after the injection of 1.5 M brine and after the 0.3 M brine. The 7 μm/voxel spatial resolution is not wide enough to notice the oil film, however, the macro details of the aqueous solutions can be inferred by visual inspection.

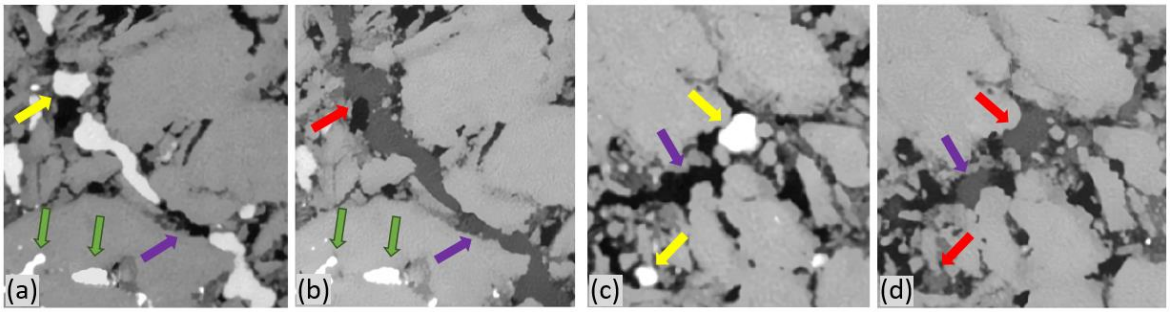

Figure 2: Regions of interest after 1.5 M brine injection (a and c, slice number 118, z direction) and the same slices after 0.3 M brine injection (b and d, slice number 208, z direction).

The high salinity solution with a contact angle lower than 90° with the rock can be observed in Figure 2 “a” and “c” (yellow arrows), indicating the oil wettability of the system. The red arrow in Figure 2b reveals a different behavior of the 0.3 M brine with and contact angle higher than 90° with the rock. This indicates a reversal in the affinity of the system induced by 0.3 M brine injection, turning the rock more wettable to the aqueous solution in that region. The purple arrows point out that the 0.3 M brine detached the oil from those constrictions and replaced the oil, it also increased the contact interface between rock and aqueous solution. In Figure 2b is also possible to notice 1.5 M brine trapped in some pores (green arrows), this suggests that the remobilization induced by 0.3 M brine clogged some interstices with oil, preventing the different solutions to blend. In Figure 2 “c” and “d”, besides 0.3 M brine replacing oil, it also shows low salinity solution (red arrows) replacing 1.5 M brine (yellow arrows). The purple arrow in Figure 2d point out a thick oil film between the rock and 0.3 M brine droplet, this indicates that, in that region, the affinity of the rock with oil is still happening. Even 0.3 M brine has replaced the oil in many places, the system is indeed mixed wet, with regions with more affinity to the aqueous solutions, whereas other regions are still wettable to the oil.

As can be noticed in the details of Figure 2, the configuration of both aqueous solutions is quite different in a system initially with more affinity with oil. In order to evaluate the influence of the low salinity solution in the wettability of the system from a wider perspective, the clusters of oil were investigated. This investigation was carried out with the 15 μm/voxel spatial resolution images in 3D.

Figure 3 shows 3D representations of the porous structure of the sample and the oil clusters configurations inside the rock. Figure 3a represents the solid phase in yellow and pore phase in blue. It is possible to notice big transparent indentations in the surface of the sample, these places are originally filled with resin and were not computed in the quantifications. Figure 3b presents the oil clusters after aging process in which disconnected clusters are depicted by different colors, rock and aqueous solutions are transparent. The largest oil cluster (red) was isolated in the Figure 3c for investigation. The volume of this cluster is 5.49 x 10^{-2} ml, 59 % of the total oil amount initially present in the porous medium (9.32 x 10^{-2} ml). After the 1.5 M brine injection (Figure 3d) minor changings can be visually noticed in the configuration of the largest connected cluster. This means that some oil remobilization was induced by high salinity solution. In fact, the volume of the red cluster increased to 7.83 x 10^{-2} ml. After 0.3 M brine is injected in the system, the configuration is quite different (Figure 3e). The volume of largest cluster is now 9.03 x 10^{-3} ml, just 12 % of the previous largest cluster volume. The 0.3 M brine, besides displacing oil to other places inside the rock (Figure 2), which indicates the detachment of the oil from the pore walls, it also disconnected the oil clusters. The disconnecting result of the largest oil cluster can be seen in Figure 3f, in which the larger oil clusters formed after 0.3 M brine injection are shown (just for clusters with volumes > 3.84 x 10^{-2} ml), the red cluster can still be seen in the bottom center of the figure. Figure 3f depicts the dismembering of oil cluster and also oil remobilization induced by low salinity solution. This oil configuration, detached from the rock and divided into several disconnected clusters, makes feasible the extraction of more oil from the system.

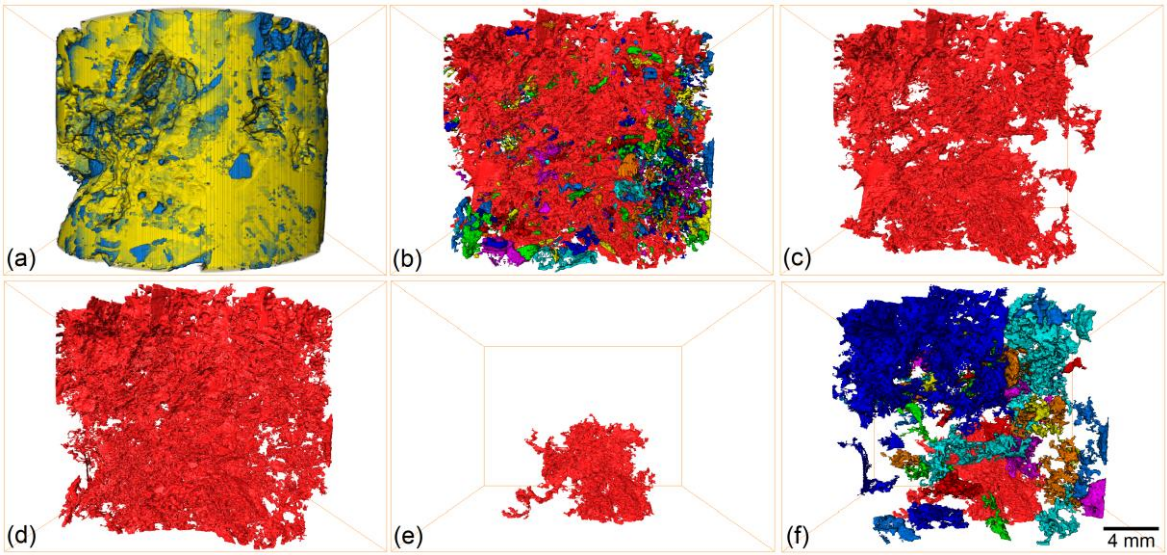

Figure 3: 3D renderings of the sample (a) with solid phase in yellow and pore phase in blue. In (b) the clusters of oil are depicted in different colors after aging process. The largest cluster from (b) is isolated in (c). The largest clusters after 1.5 M brine (d) and after 0.3 M brine injections (e). The largest cluster in red and the larger cluster in different colors after 0.3 M brine injection (f).

The oil saturation before and after aging process, and the residual oil saturation after both aqueous solutions injections were determined for each 2D slices of the tomography acquisitions, the values are displayed in the graph (Oil Saturation *versus* 2D Slice) of the Figure 4. Slice #0 is the bottom of the sample.

The difference between “before aging” and “after aging” lines indicates that the oil moved inside the sample during the thermal process. A small oil displacement induced by the aging process can be noticed after slice #250. The thermal process, besides decreasing the oil viscosity, also increases the affinity of the system with the oleic phase. Therefore, the oil tends to move towards the pore walls, causing small remobilization.

The oil saturation increased before slice #110 and after slice #360 after 1.5 M brine injection. This is a contradiction since no extra oil was injected into the sample. This oil probably was displaced from the bottom of the sample, once just the middle part of the 3D image was analysed. Either way, even though high salinity injection did not change the wettability of the system (Figure 2), it indeed interfered in the oil configuration.

The oil remobilization is more pronounced after low salinity solution injection, in which the residual oil saturation severely decreased 46.5 % (from 7.83 x 10^{-2} ml to 9.30 x 10^{-3} ml). The 0.3 M brine solution reduced the capillary forces that kept the oil trapped in the porous system and also kept the oil consolidated in a large cluster and decreased its saturation. Both lines (1.5 M and 0.3 M brines) are quite similar, presenting equivalent trends, in which the peaks and troughs are in similar positions on the graph. These peaks, which means higher saturation, are regions more suitable for oil accumulation.

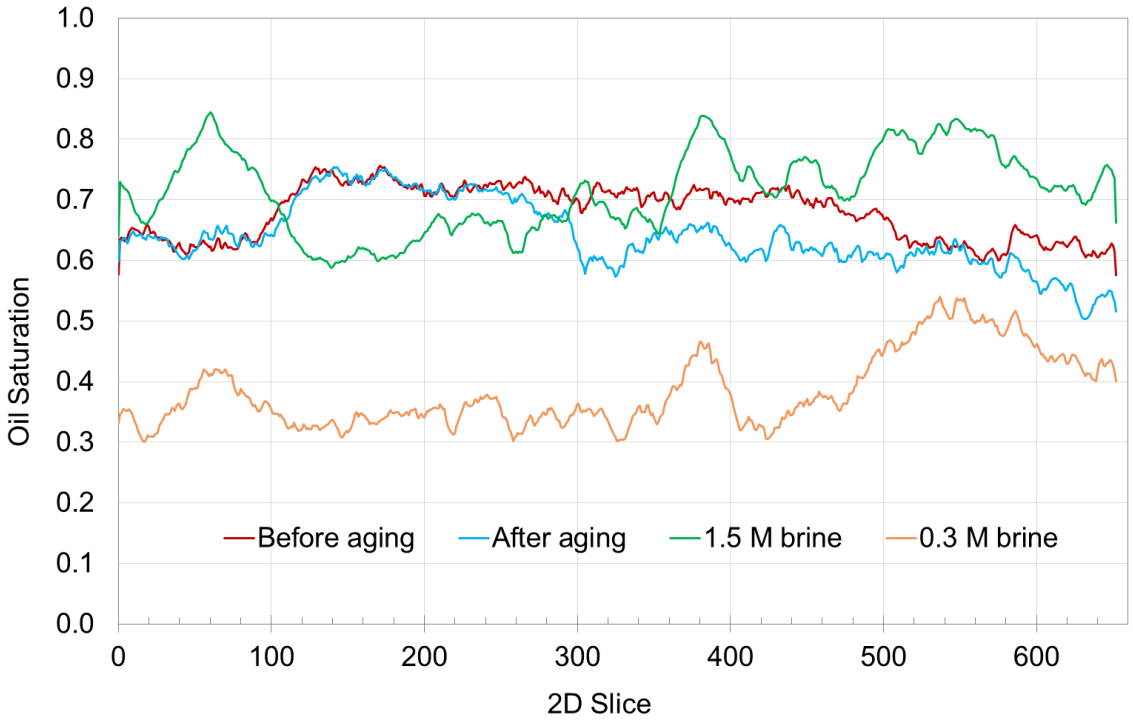

Figure 4: Oil saturation in each 2D slice along the sample after steps carried out in the experiment.

Both aqueous solutions were prepared with the same salt, however, the lowering of the ionic concentration made it capable of interfering in the wettability of the system, even after the aging process. The mechanisms behind oil remobilization induced by low salinity solution are not totally understood, however, in this experiment the 0.3 M brine was able to reverse the wettability of the system, decrease capillary forces remobilizing the oil and disjoined large oil clusters by the reduction in the interfacial tension.

5. Conclusions

In this study, an experiment of enhanced oil recovery based on low salinity water injection (LSW) was carried out using KI as an ionic compound. A carbonate rock as a storage porous medium was used and dodecane with stearic acid was the oleic phase. The experiment was monitored and analyzed with X-ray microtomography. The aging process was carried out aiming to increase the wettability of the system to the oil.

With microCT 2D and 3D images was possible, besides to observe the oil configuration inside the pore medium of the rock, also to investigate the behavior of the 1.5 M and 0.3 M brine solutions after their injections. It was possible to observe that the high salinity solution did not interfere in the affinity of the system to the oil, however, the low salinity solution reversed the wettability in many regions of the sample, spreading over the pore walls and increased the contact interface between the solution and the rock. The 0.3 M brine was able to dilute 1.5 M in many places, even though some high salinity solution remained unchanged, probably due to clogging of some interstices by oil. Low salinity solution also disjoined large oil clusters, due to the decreasing in the interfacial tension, and decreased capillary forces resulting in a significant oil remobilized, reducing in 46 % the oil saturation. The response of the analyzed rock sample to the low salinity injection can be considered positive, taking into account the reduction in oil saturation, however, it is unpredictable to state that the application of the technique will succeed for other samples with different lithologies. According to Shabaninejad et al. (2015), the same kind of experiment was applied in a sandstone sample without changing on oil recovery.

The prominent reduction in oil saturation inside the carbonate sample is in agreement with other studies focused on enhanced oil recovery as reviewed by Katende and Sagala (2019) and Al-Shalabi and Sepehrnoori (2016),

however, this high reduction suggests that low salinity water solution injection is also a promising technique that can be applied to remove oil from solid surfaces for combating oil pollution purposes.

Acknowledgments

The authors thank CENPES/PETROBRAS for the financial support to the research carried out at LMPT/UFSC; CNPq and CAPES for financially supporting the students.

References

Aladasani A., Bai B., Wu Y.S., Salehi S., 2014, Studying Low-Salinity Waterflooding Recovery Effectsin Sandstone Reservoirs, Journal of Petroleum Science and Engineering, 120, 39-51.

Almeida F., Rocha E Silva N., Souza T., Almeida D., Luna J., Farias C.B.B., Rufino R., Sarubbo L., 2019, Surfactant Activity of Artocarpus Heterophyllu Fruit Extract and Application in Oil Removal of Solid Surface, Chemical Engineering Transactions, 74,1135-1140.

Al-Shalabi E.W., Sepehrnoori K., 2016, A Comprehensive Review of Low Salinity/Engineered Water Injections and Their Applications in Sandstone and Carbonate Rocks, Journal of Petroleum Science and Engineering, 139, 137-161.

Armostrong R.T., Wildenschild D., 2012, Microbial Enhanced Oil Recovery in Fractional-Wet Systems: A Pore-Scale Investigation, Transport in Porous Media, 92, 819-835.

Bartels W.B., Rücker M., Berg S., Mahani H., Georgiadis A., Brusse N., Coorn A., van der Linde H., Fadili A., Hinz C., Jacob A., Wagner C., Henkel S., Enzmann F., Bonnin A., Stampanoni M., Ott H., Blunt M., Hassanizadeh S.M., 2016, Micro-CT study of the Impact of Low Salinity Waterflooding on the pore-scale fluid distribution during flow, SCA2016-Temp117, 12.

Duffy J.J., Peake E., Mohtadi M.F., 1980, Oil Spills on Land as Potential Sources of Groundwater Contamination, Enviromental International, 3, 107-120.

Durval I.B., Resende A., Ostendorf T., Oliveira K.G.O., Luna J., Rufino R., Sarubbo L., 2019, Application of Bacillus Cereus Ucp 1615 Biosurfactant for Increase Dispersion and Removal of Motor Oil from Contaminated Seawater, Chemical Engineering Transactions, 74, 319-324.

Gbadamosi A.O., Junin R., Manan M.A., Agi A., Yusuff A.S., 2019, An Overview of Chemical Enhanced Oil Recovery: Recent Advances and Prospects, International Nano Letters, 9171-202

Katende A., Sagala F., 2019, A Critical Review of Low Salinity Water Flooding: Mechanism, Laboratory and Field Application, Journal of Molecular Liquids, 278, 627-649.

Macheca A.D., Uwiragiye B., 2020, Application of Nanotechnology in Oil and Gas Industry: Synthesis and Characterization of Organo-modified Bentonite from Boane Deposit and its Application in Produced Water Treatment, Chemical Engineering Transactions, 81, 1091-1086.

Mantovani I.F., Coser L., Calado C.M.B., Bellini O.J., Hotza D., Quadri M.G.N., Fernandes C.P., 2019, Predicting Intrinsic Permeability of a Double Porosity Cellular Ceramic using X-Ray Micro-Tomography, Chemical Engineering Transactions, 74, 1069-1074.

Pak T., Archilha N.L., Mantovanni I.F., Moreira A.C., Butler I.B., 2018, The Dynamics of Nanoparticle enhanced Fluid Displacement in Porous Media - A Pore-scale Study, Scientific Reports, 8, 11148.

Pichtel J., 2016, Oil and Gas Production Wasterwater: Soil Contamination and Pollution Prevention, Applied and Environmental Soil Science, 2016, Article ID 2707989, 24.

Qin Z., Arshadi M., Pirl M., 2019, Micro-scale experimental investigations of multiphase flow in oil-wet carbonates. II. Tertiary gas injection and WAG,Fuel, 257, 116012.

Satter A., Iqbal G.M., 2016, Enhanced oil recovery processes: thermal, chemical, and miscible floods, Reservoir Engineering; The Fundamentals, Simulation, and Management of Conventional and Unconventional Recoveries, Elservier, 17, 313-337.

Scheffer K., Méheust Y., Carvalho M.S., Mauricio M.H.P., Paciornik S., 2020, Enhancement of Oil Recovery by Emulsion Injection: A Pore Scale Analysis From X-Ray Micro-Tomography Measurements, Journal of Petroleum Science and Engineering, 108134.

Shabaninejad M., Marathe R., Middleton J., Fogdenet A., 2015, Micro-CT pore-scale analysis of low salinity recovery from reservoir sandstones. In: 77th EAGE Conference and Exhibition 2015.

Villarraga-Gómez H., Smith, S., 2015, Optimal Specimen Orientation in Cone-Beam X-Ray CT Systems (For Dimensional Metrology). In: paper presented at 30th ASPE Annual Meeting, Austin, TX, vol. 62.

Wenguo M., 2016, The Study of Effect of Pore Structure on Oil Displacement Efficiencyof Polymer Flooding, The Open Fuels & Energy Science Journal, 9, 55-64.